Article

ACS AUTHORCHOICE

Mixed Matrix Membranes Based on Fluoropolymers with *m*- and *p*-Terphenyl Fragments for Gas Separation Applications

Hugo Hernández-Martínez, Eduardo Coutino-Gonzalez,* Fabricio Espejel-Ayala,
Francisco Alberto Ruiz-Treviño, Gabriel Guerrero-Heredia, Ana Laura García-Riego,
and Lilian Irais Olvera*

Read Online

ACCESS | Metrics & More | Article Recommendations | Supporting Information

ABSTRACT: Novel mixed matrix membranes (MMMs) based on fluoropolymers with *m*- and *p*-terphenyl fragments and NaX zeolites were prepared. The fluoropolymers were synthesized by a one-pot, room-temperature, metal-free superacid-catalyzed stoichiometric and nonstoichiometric step polymerization of 2,2,2-trifluoroacetophenone with two multiring aromatic nonactivated hydrocarbons (*p*-terphenyl and *m*-terphenyl). MMMs were characterized by scanning electron microscopy (SEM) and infrared (Fourier transform infrared (FTIR)) spectroscopy and used in gas permeability tests. SEM analysis showed interfacial voids in MMMs prepared in *N*-methyl-2-pyrrolidone (NMP), The interfacial adhesion in the polymer−zeolite system was considerably improved when chloroform was used as a solvent. Permeability coefficients for pristine polymer membranes were 1.3-fold higher in $CHCl_3$ than in NMP for *p*-terphenyl fragment and 2.0 times higher in NMP than in $CHCl_3$ for the polymer with *m*-terphenyl fragment. The incorporation of NaX zeolites in the polymeric matrices improved the gas permeability coefficients compared to the pristine membranes. The effects of polymer architecture, casting solvent, and interaction between the organic matrix and the inorganic particles on the gas separation performance of the developed MMMs were investigated.
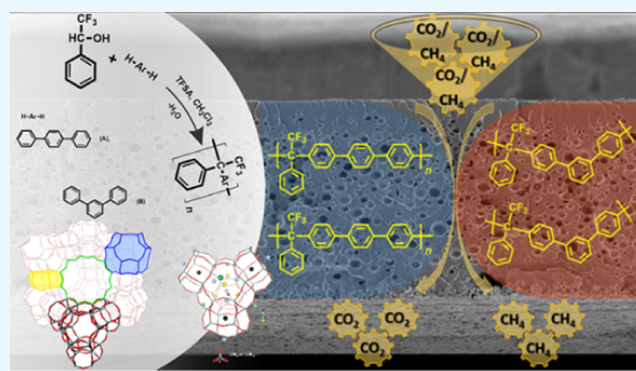
INTRODUCTION

Membrane science and technology has been identified as a powerful tool in solving relevant industrial problems required for a sustainable growth,[1,2] for instance, in greenhouse gases (GHG) capture and separation processes. Gas separation membranes present important advantages such as high separation performance, low cost, flexible operation, low energy requirement, and the ability to make sheets or modules.[1,3] The gas separation properties of membranes depend on different factors such as material, thickness, configuration (flat, hollow fiber), as well as the module/system design.[1] However, the main limitation of gas separation membranes is the permeability-selectivity trade-off since membranes with a high gas permeability usually display low selectivity and vice versa, as exemplified by the Robeson's upper bound.[4]

An alternative to improve the separation performance of polymeric membranes is to incorporate specific microporous adsorbents or molecular sieves, such as zeolites, as fillers into the polymeric matrix.[5] As a result, new technologies such as mixed matrix membranes (MMMs) have emerged with tailored separation properties.[6,7] The concept of MMM combines the advantages of each phase; high selectivity of

the inorganic phase and desirable mechanical properties and feasible processability of polymers.[8,9] The gas permeability through MMMs depends on several factors such as intrinsic properties of filler and polymer, the filler−polymer matrix interface, and the filler loading,[5] ideally resulting in membranes with properties that exceed the "upper bound".[9−12]

In this study, the development, characterization, and performance of MMMs based on two fluorinated aromatic polymeric matrices with *m*- and *p*-terphenyl fragments, as well as NaX zeolites (highly attractive zeolite topology employed in gas separation and/or purification processes[13]) were explored. NaX zeolites comprise aluminosilicates that combine a three-dimensional network of accessible microporous[14−16] with a diameter of 0.74 nm and conventionally compact (cub)-octahedral crystal morphology.[15] On the other hand, aromatic fluoropolymers have received special attention in the last three

decades mainly for their unique properties and high-temperature performance. The use of fluorine-containing groups in macromolecules increases polymer solubility, glass-transition temperature, thermal stability, and chemical resistance.[17,18] Many amorphous glassy perfluorinated polymers have large free volume, great gas permeability, and can be considered as efficient materials for gas separation membranes.[19] Although this kind of polymers have been used in gas separation applications, it is important to mention that fluoro-containing monomers for polymer syntheses are expensive, and consequently only few are commercially available. Therefore, simple and reliable synthesis of aromatic fluoropolymers would be of paramount importance to overcome this limitation. The polymer synthesis presented in this work involves a Friedel–Crafts polycondensation reaction in a superacid medium of a fluorinated carbonyl compound (2,2,2-trifluoroacetophenone 1a) with two multiring aromatic nonactivated *p*-terphenyl **A** and *m*-terphenyl **B**.[18]

RESULTS AND DISCUSSION

Polymer Synthesis. Polymer synthesis was carried out by a one-pot, room-temperature, metal-free superacid-catalyzed stoichiometric and nonstoichiometric step polymerization of a fluorinated carbonyl compound (2,2,2-trifluoroacetophenone) 1a with two multiring aromatic nonactivated hydrocarbons (*p*-terphenyl and *m*-terphenyl). It is known that the classical theory of polycondensation is based on two main principles, one is the requirement of stoichiometry between monomers.[20] Under this condition, polymers with high molecular weights have been obtained. However, the synthesis of linear, high- or ultrahigh-molecular-weight polymers by nonstoichiometric superacid-catalyzed polyhydroxyalkylations has been recently reported.[18,21]

Remarkably, the reactions proceed with an increase in the reaction rate and a decrease in the macrocycles fraction. Also, even under nonstoichiometric conditions, monomers with low reactivity or purity could be polymerized with good yield. Taking into account that terphenyl and some fluorinated ketones have moderate reactivity, reactions were conducted under both stoichiometric and nonstoichiometric conditions, according to the reactions depicted in Scheme 1. The polymer 2aA was obtained according to the methodology already reported.[18] The synthesis of polymer 2aB was performed by
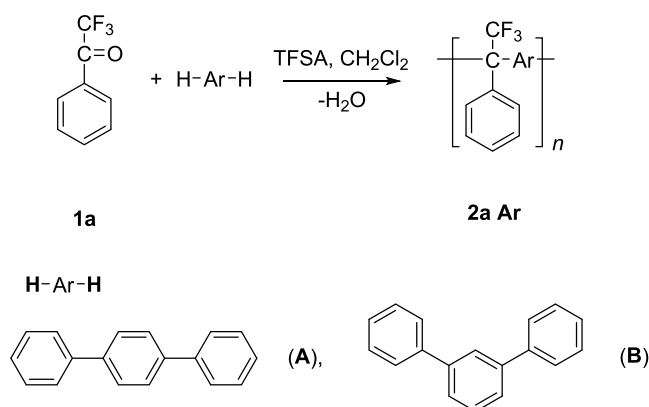
nonstoichiometric polycondensation with a 20% excess of 1a (2,2,2-trifluoroacetophenone) in a homogeneous phase.

NMR analysis was possible due to the high solubility of the polymers obtained. It is noteworthy that it is difficult to achieve high regioselectivities in polyhydroxyalkylations via a Friedel–Crafts-type reaction. However, the NMR studies revealed only *para* substitutions in the phenylene fragment. The NMR analysis of polymer 2aA presented highly resolved patterns with no evidence of structural irregularities or evidence of *ortho* or *meta* substitutions (Figure 1). The reaction with *meta*-terphenyl (2aB) resulted in polymers with kinked structures; this is an efficient way to alter the conformation and architecture of polymer chains generating additional folding. Spectral analysis of the obtained polymer 2aB by NMR did not reveal any structural irregularities or the presence of isomers (Figure 2). It is a general belief that the signals in ^{1}H NMR spectra of wholly aromatic polymers with high molecular weights are wide; therefore, it is worth noting that all of the spectra obtained display sharp signals and highly resolved patterns and all of the anticipated resonances are evident, confirming the high regioselectivity of the superacid-catalyzed polyhydroxyalkylation reactions performed (Figures 1 and 2).

Membrane Formation and Characterization. MMMs obtained from two polymeric matrices (2aA and 2aB) and NaX zeolites represent the first attempt to develop alternative materials for gas separation applications using wholly aromatic fluoropolymers with rigid ether-bond-free aryl backbones. It is expected that the comparison between both matrices (containing *p*-terphenyl and *m*-terphenyl fragments) will set the basis to establish certain property–structure relationships depending on the polymer chain rigidity or the conformation imposed by rigid segments; in the case of polymer 2aA, higher chain stiffness is expected due to the rigid *p*-terphenyl fragments, while the 2aB polymer presents twisted structures and less degree of stiffness when *m*-terphenyl is used as an aromatic compound for the formation of macromolecules. Materials with rigid segments restricting the mobility usually exhibit good separation parameters. On the other hand, one of the main factors affecting the performance of MMMs is the interaction and compatibility of the two components of different nature (polymer and zeolite); this way the right choice of solvents that could favor the polymer–zeolite interaction is relevant. The development of MMMs from these polymeric matrices and zeolites provides a first approximation for the implementation of novel fluorinated materials with high chemical, mechanical, and thermal stabilities, and commercial zeolites with high separation performance in membranes for gas separation technologies.

Fourier Transform Infrared (FTIR) Spectra. The characterization of the obtained materials was carried out by FT-IR spectroscopy, the spectra of the neat fluoropolymers 2aA and 2aB, as well as MMMs are shown in Figure 3. The pristine polymeric membranes displayed an absorption band at 3035 cm^{-1} attributed to the C–H stretching; meanwhile, the appearance of two bands at 1225 and 1149 cm^{-1} corresponds to the C–F stretching, and the bands at 1490 and 810 cm^{-1} are attributed to the C–C aromatic stretching.[18] All of the MMM samples displayed the characteristic peaks at 450, 560, and 960 cm^{-1} associated with O–Si–O, Al–O–Si, and Si–O vibrations typically encountered in zeolite materials.[7] The peak between 1600 and 1700 cm^{-1} in the 2aA-NaX4 and 2aB-NaX4 membranes is attributed to the OH stretching and bending

Scheme 1. Step Polymerization of 2,2,2-Trifluoroacetophenone with Two Multiring Aromatic Nonactivated *p*-Terphenyl (A) and *m*-Terphenyl (B)

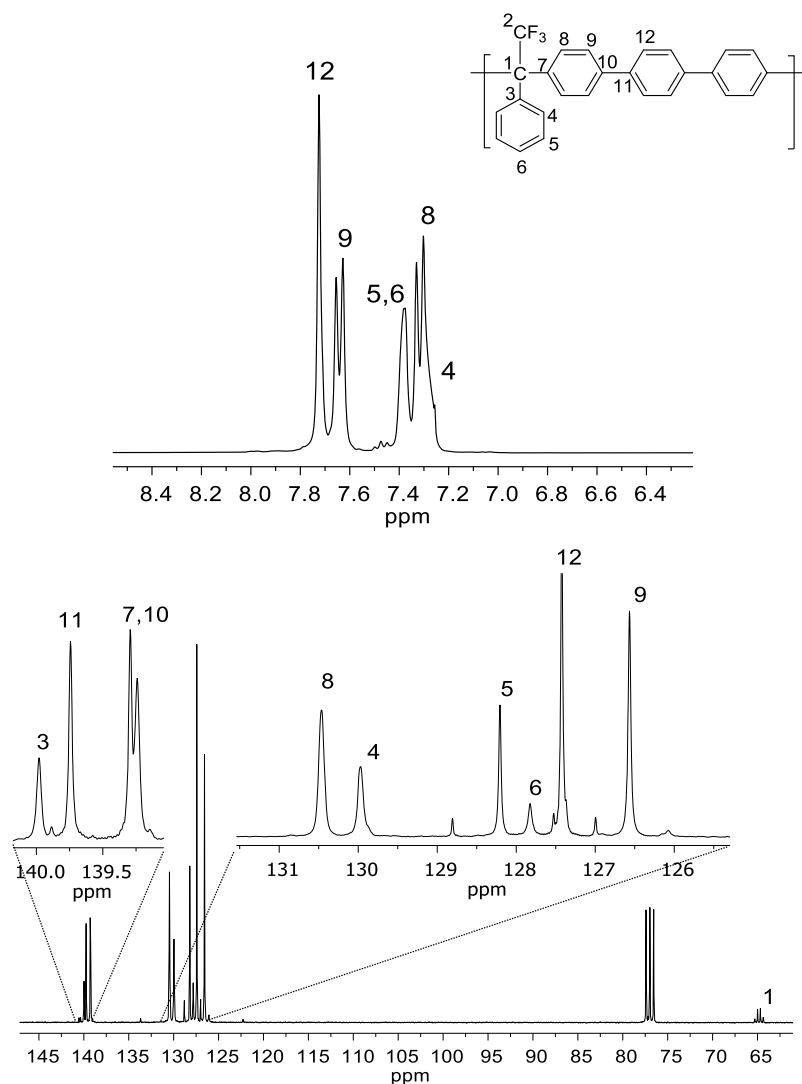**Figure 1.** ^{1}H (top) and ^{13}C NMR (bottom) spectra of polymer 2aA.

modes of the water molecules adsorbed by the zeolite.[22,23] Also, in all MMMs, a broad band centered at around 3248 cm^{-1} was observed, which could correspond to the water present in the zeolites.

Scanning Electron Microscopy (SEM) Analysis. Scanning electron microscopy was conducted to investigate the morphology of MMMs. Figure S1 (Supporting Information) shows the SEM micrograph of NaX zeolites, which exhibit a polyhedral geometry, typical of this kind of zeolite with size distribution between 2 and 5 μm. Figure 4 shows the SEM images of dense membranes made of 2aA (Figure 4a) and 2aB (Figure 4b) in *N*-methyl-2-pyrrolidone (NMP), where the cross section of both membranes displays a homogeneous phase and defect-free morphology. Micrographs of MMMs based on the two polymer matrices 2aA-NaX4 and 2aB-NaX4 in NMP and CHCl$_3$ are depicted in Figure 4c−f, respectively.

Figure 4c shows an irregular morphology with interfacial voids in the 2aA-NaX4 membranes. This kind of morphology is evidence of poor adhesion between the polymer and the zeolite particles. This feature shows the incompatibility of the polymer−zeolite system and leads to the formation of nonselective voids at the interphase regardless of the zeolite type.[24,25]

2aB-NaX4 MMM in Figure 4d displays the same morphology as that of the 2aA-NaX4 membrane (Figure 4c), where porous structures with very marked interfacial voids were observed, indicating poor interfacial adhesion. In addition, particle agglomeration on the surface can also be observed (Figure S2). This observation indicates that this particular type of zeolite has low compatibility in the polymer−zeolite interface when NMP is used as a solvent, probably due to the greater affinity of NMP toward the polymer than the zeolite. It is known that one of the main factors affecting the interaction and compatibility of two components of different natures (polymer and zeolite) in MMMs is the solvent.[26] Also, according to Mahajan et al.,[27] the nature of the polymer−zeolite components and the stress encountered during material preparation are two critical factors in the formation of the interphase. The MMMs were prepared using NMP as a solvent, which requires a conventional oven and relatively long times to achieve complete evaporation generating stress conditions (created during the solvent evaporation at 80 °C for long periods), which could lead to interfacial voids. The morphology observed in the MMMs is typical of an incompatible polymer−zeolite system, and the formation of voids at the interphase is known as sieve-in-a-cage morphology,
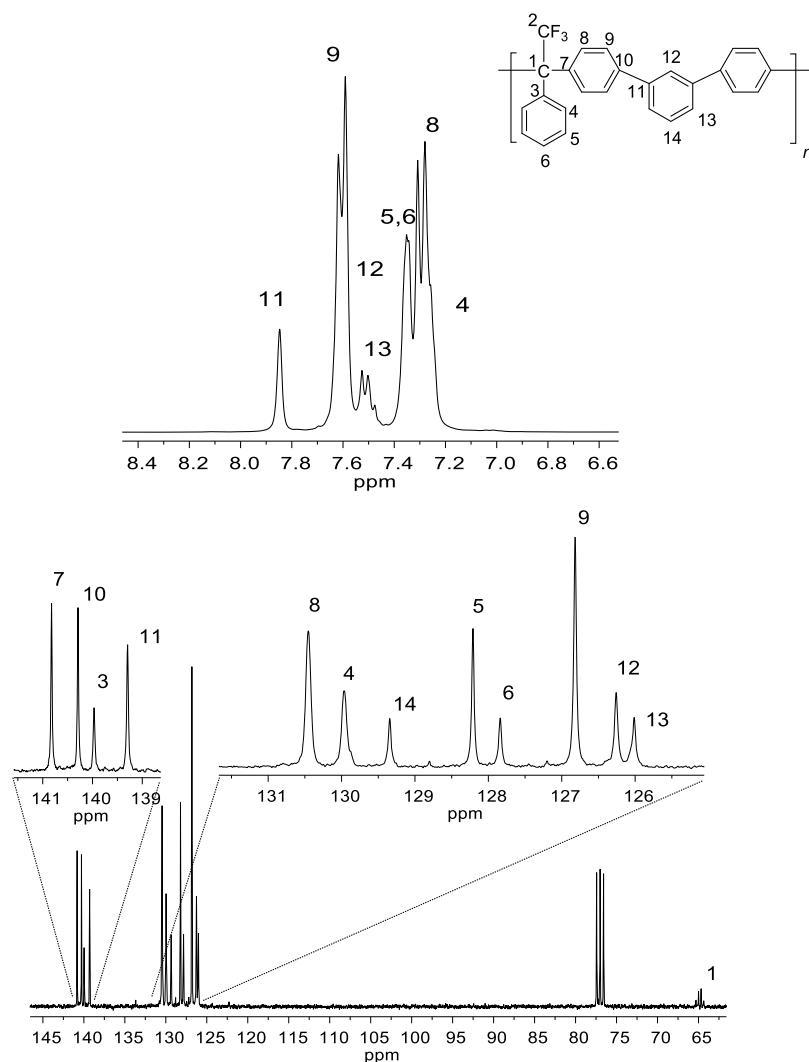
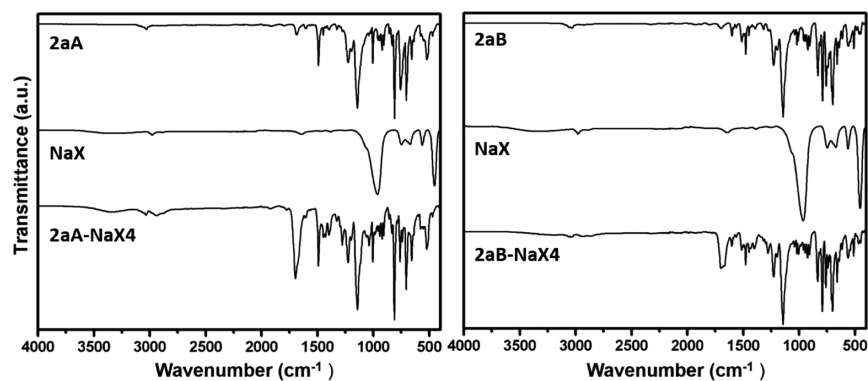**Figure 2.** ¹H (top) and ¹³C NMR (bottom) spectra of polymer 2aB.

Figure 3. FT-IR spectra of the neat fluoropolymers 2aA and 2aB, as well as MMMs.

which has considerable effects on the performance of MMMs, for example, high permeability and low selectivity.[23]

To increase the degree of adhesion between the zeolite–polymer interfaces, MMMs were prepared using chloroform as a solvent, which decreases the stress conditions during the solvent evaporation step since the evaporation process during the fabrication of the MMMs takes place at room temperature and at relatively short times, compared to those prepared in NMP. Figure 4e,f displays the SEM cross section analysis of

2aA-NaX4 and 2aB-NaX4 obtained with chloroform. The interfacial adhesion in the polymer–zeolite system was considerably improved when chloroform was used as a solvent. In addition, a better distribution of zeolite particles in the polymer matrix was observed generating greater compatibility between the components of the MMMs. Direct comparison between the membranes obtained under chloroform and NMP (Figure 4c vs e, d vs f) confirms these observations. It is important to mention that both solvents (CHCl₃ and NMP)
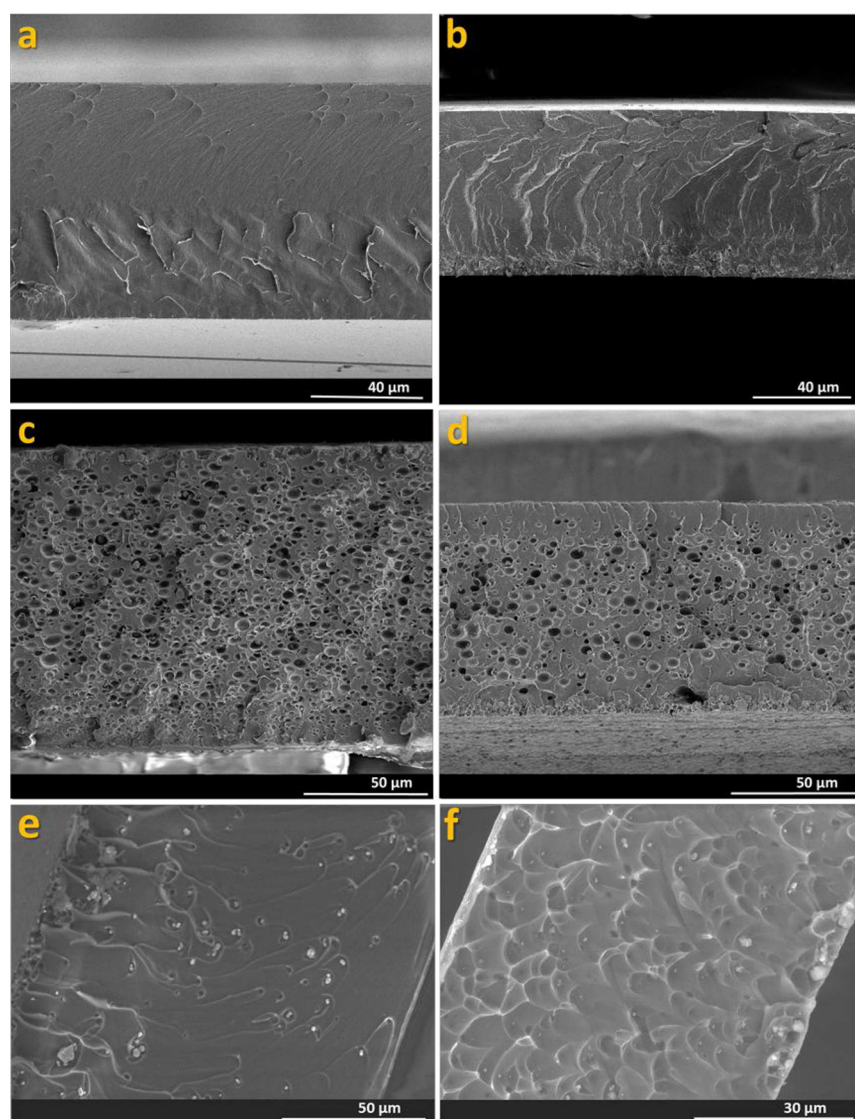
Figure 4. SEM micrographs of the cross section of dense polymeric membranes and MMMs prepared in NMP: (a) 2aA, (b) 2aB, (c) 2aA-NaX4, and (d) 2aB-NaX4, as well as MMMs prepared in CHCl$_3$: (e) 2aA-NaX4 and (f) 2aB-NaX4.

have a good affinity to the polymer; however, CHCl$_3$ allows a better interaction between the polymer and the zeolites due to the conditions of the membrane formation process, limiting the movement of the zeolite particles, since the evaporation rate of CHCl$_3$ is faster than that of NMP.

The presence of interfacial voids in polymer–zeolite systems has an important effect on the gas transport properties of MMMs,[28] particularly in polymers with high glass-transition temperatures, which can crack during MMM formation.[27] In this study, the developed polymeric membranes and MMMs did not display a clear tendency to fracture; this is mainly due to its high thermostability with no significant weight loss below 500 °C (under air) as observed in thermogravimetric analysis (TGA) studies (Figure 5 and Table S1), and glass-transition temperatures were not detected before its decomposition temperature. This behavior is analogous to that of similar polymers.[18,29−33] On the other hand, the obtained MMMs withstood harsh conditions during solvent evaporation (up to 200 °C, when NMP was used as a solvent) and gas transport measurements where pressures up to 2 bar were employed.

This depicts the good thermal and mechanical stabilities, at least under the conditions studied, of the obtained MMMs.

Gas Permeability Results. Table 1 shows the permeability coefficients for pure gases (H$_2$, O$_2$, CO$_2$) in 2aA and 2aB polymeric membranes as well as their respective membranes modified with NaX zeolites, at 35 °C and 2 bar, the ideal selectivity for some gas pairs, the specific volume, and their fractional free volume (FFV), to study the performance of pristine polymer membranes (based on aromatic fluoropolymers) and some MMMs formed with zeolites.

The different units of *m*- and *p*-terphenyl in the fluoropolymer backbones affect the conformation and morphology, and thus are expected to have an impact on the gas transport properties of their membranes via the modification of their fractional free volume. Specifically, the different connectivities of repeating units between *meta*- and *para*-terphenyl could lead to different chain packing due to the chain rigidity in the conformation of polymer chains imposed by rigid segments. A three-dimensional (3D) model studied by Chulsung Bae et al.,[36] in which polymers very similar to those here synthesized were investigated, suggested that *meta*-
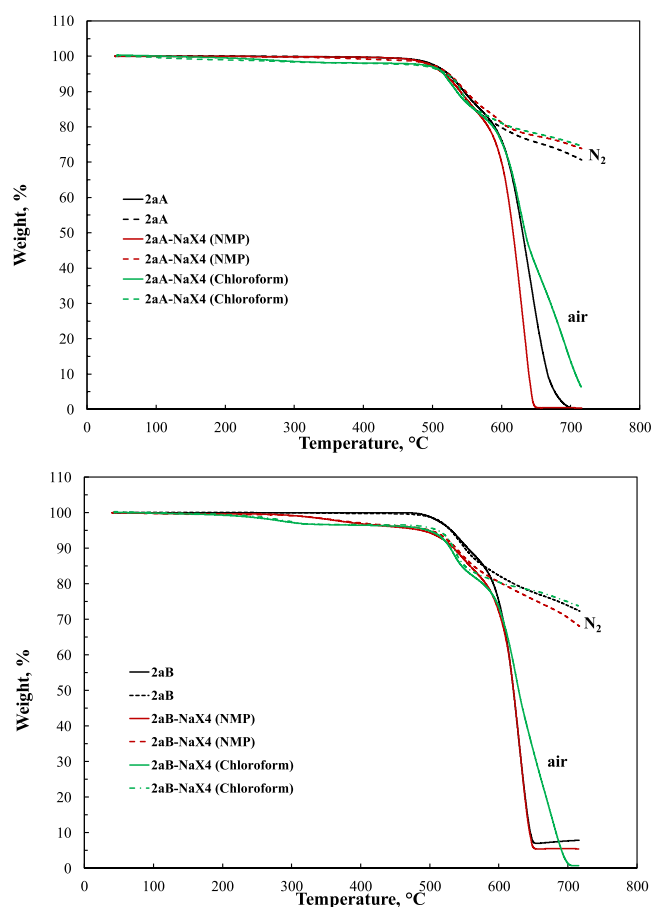
Figure 5. TGA thermograms of the membranes of polymer 2aA (top) and 2aB (bottom).

connectivity of terphenyl units allows the polymer chains to fold back to maximize the interaction between hydrocarbon backbones, while the backbone chains of *para*-terphenyl tend to spread out to prevent such conformation. The fold back chains from *meta*-fragment allow the formation of more compact polymer packing. For all measured gases (except for H_2 in NMP), polymer membranes 2aA that possesses a more rigid structure imposed by the *para* position, exhibit higher gas permeability coefficients compared to the polymer membranes 2aB, which present a twisted structure and thus a more compact polymer packing. The gas permeability coefficients of

neat polymers also correlate with their FFV since polymer 2aA exhibits a higher FFV (0.192) than polymer 2aB (0.176). Interestingly, the permeability coefficients and the FFV of neat polymer membranes also correlate with the polymer chain packing imposed by the *meta* or *para* connectivity according to the 3D models suggested for these types of conformations.[36]

In general, for the membrane 2aB, the gas permeability coefficients follow the order $P(H_2) > P(CO_2) > P(O_2)$, which is governed by the molecular size and kinetic diameter parameters. This behavior is in agreement with the apparent diffusivity of H_2, which is higher than CO_2 (Table S2). Based on this observation, the permeability coefficients for 2aB polymeric membranes are predominantly dominated by the size of permeants. In contrast, for the 2aA membrane (in both solvents), the permeability of the gases follows the order $P(CO_2) > P(H_2) > P(O_2)$. In this case, the CO_2 permeability is greater than that of H_2 due to its solubility coefficient in both solvents, NMP and $CHCl_3$, which is higher in all cases (Table S3). Thus, the permeability coefficients for 2aA polymeric membranes are dominated by the gas solubility coefficients. A similar behavior was reported by Murali and collaborators,[37] using Pebax and X-Pebax membranes in which they attributed the CO_2 permeability to the greater solubility of CO_2 in Pebax polymer, which is, to a certain extent, inert to the other gases.

Although this behavior is similar for both solvents in each polymer (Table 1), there is a difference in the permeability coefficients for both membranes caused by the effect of solvent casting. This difference is due to the gas solubility in the membrane, while the solubility coefficients are higher in membrane 2aA in $CHCl_3$ than in NMP; the opposite effect was observed in the case of membrane 2aB for all measured gases (Table S3). On the other hand, it is known that the chain stiffness could induce relatively low gas permeability and high selectivities,[38] and the flexible movements of the polymer chains are favorable for the transport of gas molecules.[35] In our case, the 2aA polymer displays high gas permeability, but no large increases in selectivity could be observed compared with the kinked structures encountered in membrane 2aB. Banerjee and collaborators[39] reported a similar behavior with polymers containing rigid terphenyl units.

Another factor contributing to the gas permeability performance is the incorporation of inorganic particles, where an improvement of the gas permeability performances compared to pure polymer membranes is expected. In this study, the addition of NaX zeolites improved the gas permeability in

Table 1. Gas Permeability Coefficients and Ideal Selectivity, Measured at 35 °C and 2 Bar Upstream Pressure, as well as Specific Volume and Fractional Free Volume for Membranes Based on 2aA and 2aB Neat Polymers and Their MMMs

membrane	solvent casting	permeability coefficient,[a] $P(i)$			ideal selectivity, $P(i)/P(j)$				$V(30 °C),$[b] cm³/g	FFV
		H_2	O_2	CO_2	H_2/CH_4	O_2/N_2	CO_2/N_2	CO_2/CH_4		
2aA	NMP	30	7.5	46	10	3.6	22	16	0.835	0.192[c]
2aA	$CHCl_3$	40	9.5	50	13	3.7	19	16		
2aA-NaX4	NMP	111	31	191	9	3.5	22	15	0.820	0.203[d]
2aA-NaX4	$CHCl_3$	43	11.4	73	8	3.4	22	14		
2aB	NMP	35	5.6	28	26	4.6	23	21	0.819	0.176[c]
2aB	$CHCl_3$	17	2.6	14	26	4.8	25	21		
2aB-NaX4	NMP	61	8.6	40	31	4.8	22	20	0.804	0.183[d]
2aB-NaX4	$CHCl_3$	15	2.3	11	27	4.6	22	20		

[a]Permeability in Barrer (1 Barrer = 1×10^{-10} cm³ STP cm/cm² s cm Hg). [b]$V(30 °C)$ specific volume determined at 30 °C in a density gradient column. [c]FFV calculated as FFV = $[V(30 °C) - V(0)]/V(30 °C)$, where $V(0) = 1.3 \sum V_w$ is the occupied volume and V_w is the van der Waals volume of the repeating unit calculated from group contribution methods developed by Van Krevelen.[34] [d]FFV calculated according to ref 35.
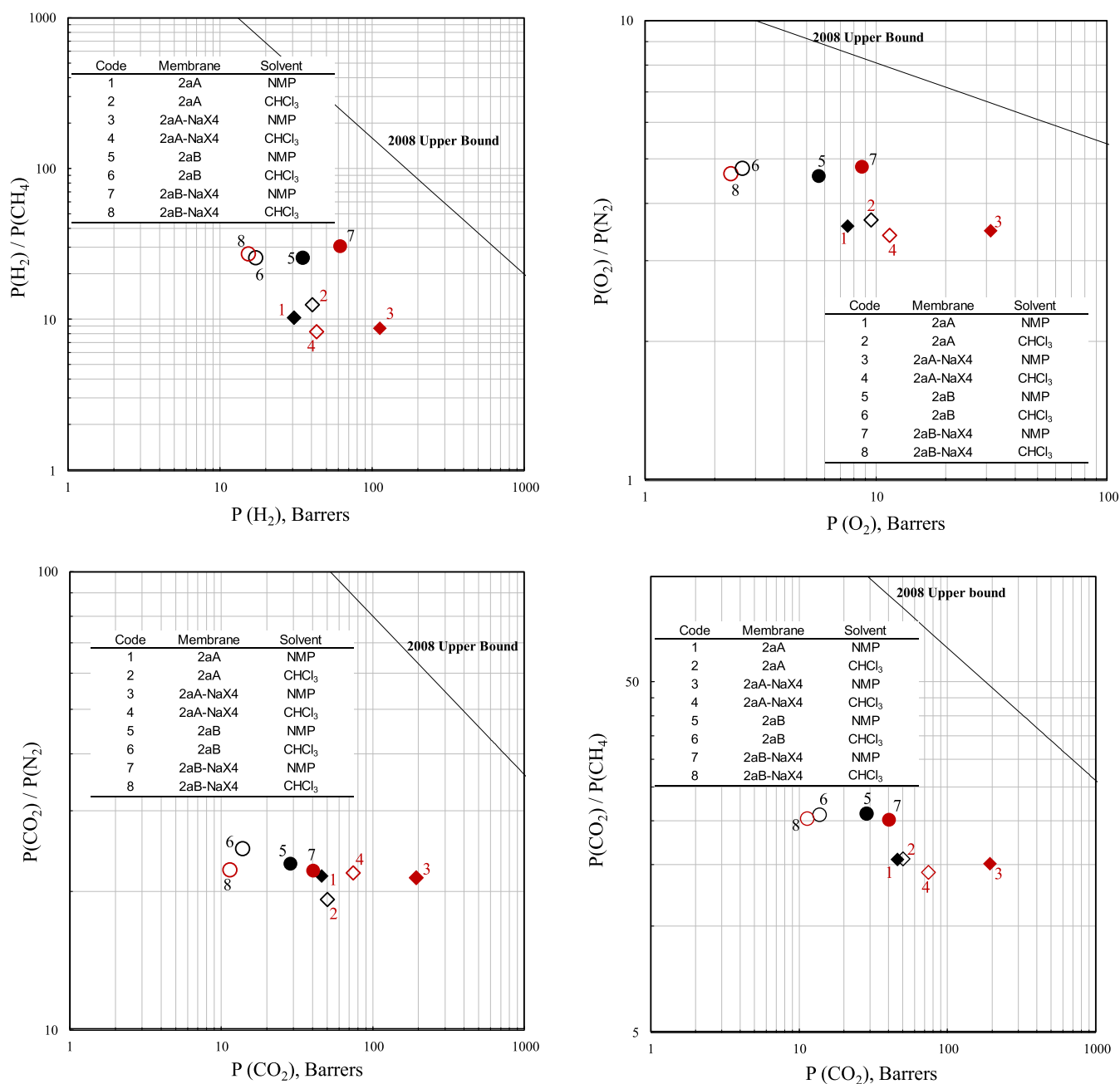
Figure 6. Ideal selectivity−permeability relationships for the gas pairs H_2/CH_4, O_2/N_2, CO_2/N_2, and CO_2/CH_4, determined for membranes based on polymers 2aA and 2aB and their respective MMMs.

almost all of the cases, as shown in Table 1. The gas permeability coefficients for all of the MMMs follow the same behavior compared to their corresponding pristine membranes in both solvents for each polymer, and the rates at which gases pass through the membrane follow the order $P(CO_2) > P(H_2)$ $> P(O_2)$ for 2aA-NaX4; and $P(H_2) > P(CO_2) > P(O_2)$, for 2aB-NaX4.

The changes in gas permeability coefficients due to zeolite addition are also associated with the solvent casting methodology, in which the major values were observed in membranes prepared in NMP. For example, the gas permeability of 2aA-NaX4 membrane (NMP) presented an increase of 75% (compared to the pristine polymer membrane) for all gases without gain in selectivity; this could be explained by the observed increase in the FFV value (0.203) compared to that

of the pristine membrane (0.192). On the other hand, in the 2aB-NaX4 membrane, the increase is less pronounced, but it has a major selectivity compared to the pristine 2aB membrane (Table 1). This membrane (2aB-NaX4) also displayed an increase in the FFV value (0.183) compared to pristine membrane (0.176). This increase in permeability is probably due to the low polymer−zeolite compatibility present in this system; in fact, the morphology observed by SEM shows interfacial voids that could directly affect the permeability. The SEM analysis for MMMs in NMP presented a sieve-in-a-cage-type morphology, favoring an increase in permeability in the same proportion for all gases, which means that the size of the interfacial voids is greater than the molecular diameter of all measured gases; this may serve as an alternative pathway for the gas molecules without making any distinction for the

molecular size, compromising the separation properties of the MMMs.[26,40]

In membranes prepared in $CHCl_3$, for instance, 2aA-NaX4, a slight increase in gas permeability of all measured gases compared to the pristine 2aA polymeric membranes was observed. The increase in permeability with respect to the pristine membrane is mainly attributed to the addition of zeolite because the solubility coefficients for this membrane are lower than that observed in the pristine membrane 2aA in $CHCl_3$. However, in the case of CO_2, the increase in permeability can be associated with a major solubility coefficient compared to other gases. The selectivity of membrane 2aA-NaX4 decreases for the H_2/CH_4, O_2/N_2, and CO_2/CH_4 gas pairs, except for CO_2/N_2, which displays a 12% increase compared to the 2aA polymeric membrane in $CHCl_3$ (Table 1). A more compact structure without interfacial voids was observed by SEM when $CHCl_3$ was used as a solvent to form MMMs, which suggests a better polymer−zeolite interaction and, consequently, the gas permeability is not affected by the presence of interfacial voids compared to the morphology observed for 2aA-NaX4 in NMP. On the other hand, although the 2aB-NaX4 membrane displayed a good polymer−zeolite interaction, according to the SEM observations, a decrease in both properties, permeability and selectivity, could be observed when $CHCl_3$ was used as a solvent, compared to the pristine 2aB membrane. Also, the decrease in CO_2 permeability was attributed to its low solubility coefficient. In general, the addition of this type of zeolites in the polymeric matrix (2aA and 2aB) provides materials with different behavior that depend on the solvent casting methodology. When NMP is used as a solvent, there is an increase in permeability, but the morphology is not the optimal (interfacial voids are formed affecting the gas transport properties). On the other hand, when $CHCl_3$ is used to obtain the MMMs, the morphology and compatibility between inorganic particles and the organic matrix was improved, suggesting that the solvent in the polymer−zeolite system has an important positive effect in the interfacial interaction to incorporate inorganic fillers in polymeric matrices, slightly improving their gas transport properties, even though they are not very significant as expected.

Figure 6 shows the selectivity−permeability plots for H_2/CH_4, O_2/N_2, CO_2/N_2, and CO_2/CH_4 gas pairs compared with the Robeson's upper bound.[4] All membranes of 2aA polymer display good permeability but slightly lower selectivity compared with membranes based on polymer 2aB, as well as exhibit typical trade-off, as shown for the H_2/CH_4, O_2/N_2, and CO_2/CH_4 gas pairs. For all gas pairs, the 2aA-NaX4 membrane displays better permeability values over other membranes obtained in this study (Table 1), and their selectivity for CO_2/N_2 gas pair is almost the same for all measured membranes, suggesting that this membrane has a good performance for this gas pair because the typical trade-off is not observed.

The results regarding the transport properties in terms of permeability and selectivity show the great potential that MMMs based on novel fluoropolymers (2aA, 2aB) and zeolites have compared to similar systems. For example, Zarshenas et al.[7] reported for the Pebax/NaX system a CO_2 permeability of 32.3 and a CO_2/N_2 selectivity of 98. This is higher than that of the MMMs presented in this study for the same gas pair (measured at 35 °C and 2 bar), but the difference lies in the operation conditions (3 bar and 25 °C) and the characteristics of the used materials (nano-zeolite NaX). Another system

reported by Azizi et al.,[41] with 4 wt % of different fillers, such as TiO_2, SiO_2, and Al_2O_3, showed similar performance in the CO_2 permeability compared to 2aA-NaX4 in NMP but lower selectivity. Although the results obtained for the membranes developed in this report are below the Robeson's upper bound, this study opens new avenues for further exploration and optimization of fluoropolymers with *m*- and *p*-terphenyl fragments in gas separation applications.

■ CONCLUSIONS

MMMs with potential use in gas separation were developed using two novel polymeric matrices, synthesized by one-pot, room-temperature, metal-free superacid-catalyzed polyconden-sation of 2,2,2-trifluoroacetophenone with multiring aromatic nonactivated hydrocarbons (*p*-terphenyl and *m*-terphenyl) and 4 wt % NaX zeolite in two solvents (NMP and $CHCl_3$), representing the first attempt to develop hybrid materials based on ether-bond-free fluoropolymers main chains. The synthesis method allows us to produce polymers with high molecular weights and form flexible and transparent membranes with good chemical, thermal, and mechanical properties to withstand pressure conditions used in permselectivity studies. The comparison of the two polymer matrices and the MMMs obtained allowed us to establish property−structure relation-ships based on the polymer structure, namely, chain rigidity or the conformation imposed by rigid segments of the polymer 2aA (*p*-terphenyl) and twisted structures with less degree of stiffness of the polymer 2aB (*m*-terphenyl). Dense membranes and MMMs were characterized by the FTIR, TGA, and SEM analyses, as well as employed in gas permeation tests. The SEM results revealed a low compatibility between NaX zeolite and fluropolymer matrices, 2aA and 2aB, in NMP, observing the presence of interfacial voids. The compatibility was improved when MMMs were prepared in $CHCl_3$. This indicates that the solvent also plays an important role in the MMMs morphology. Based on gas permeation studies, the dense membrane 2aA presented higher permeability coefficients in $CHCl_3$ than in NMP, while the opposite effect was observed in the membrane 2aB. This behavior was mainly attributed to solubility coefficients of the measured gases in both membranes. The incorporation of NaX zeolites improved the gas permeability coefficients compared to pristine membranes, which are higher in NMP than in $CHCl_3$ for both polymers used in the MMMs. Comparison of gas permeability and selectivity of similar systems with those reported in this study highlights the great potential that MMMs based on fluoropolymers and NaX zeolites display, paving the way to further explore these hybrid materials in gas separation applications.

■ EXPERIMENTAL SECTION

Materials. All starting materials purchased from Sigma-Aldrich, including 2,2,2-trifluoroacetophenone, *m*-terphenyl, and *p*-terphenyl, were used without further purification. *N*-methyl-2-pyrrolidone (NMP), chloroform ($CHCl_3$), dichloro-methane (CH_2Cl_2), and trifluoromethanesulfonic acid (TFSA) were distilled prior to use.

FAU zeolites in their sodium (FAU-NaX) form were obtained from CLARIANT. FAU-NaX, hereafter referred to as NaX, Si/Al ratio of 1.2, surface area >600 m^2/g, were employed. Table S4 and Figure S2 show the elemental

composition and the schematic representation of zeolite FAU topology, respectively.

Synthesis of Polymer 2aA (*p*-Terphenyl Fragment). Stoichiometric conditions: a mixture of 2,2,2-trifluoroacetophenone 1a, (1 mL, 0.00759 mol), *p*-terphenyl **A**, (1.7479 g, 0.00759 mol), dichloromethane (13.5 mL, 0.2114 mol), and TFSA (4.5 mL) was stirred at room temperature for 24 h. The resulting green viscous solution was poured into methanol, and the precipitated white powder was filtered, extracted with refluxing methanol, and dried overnight before reprecipitation from NMP solution into methanol to obtain a fibrous material. The resulting pure white fibrous polymer (95% yield) displays an inherent viscosity (η_{inh}) of 0.62 dL/g.[18]

Synthesis of Polymer 2aB (*m*-Terphenyl Fragment). 2,2,2-Trifluoroacetophenone 1a, (1.27 mL, 0.009108 mol, 20% excess, nonstoichiometric conditions), *m*-terphenyl **B** (1.7479 g, 0.00759 mol), dichloromethane (13.5 mL, 0.2114 mol), and TFSA (4.5 mL) were mixed under magnetic stirring for 5 h at room temperature; then, the mixture was precipitated in methanol. The white fibers obtained were washed in hot methanol twice (60 °C) and then reprecipitated from *N*-methyl-2-pyrrolidone (NMP) into methanol. The resulting pure white fibrous polymer (97.5% yield) presents an inherent viscosity (η_{inh}) of 0.52 dL/g.

Membrane Preparation. Dense neat polymer membranes (2aA and 2aB) and their respective MMMs containing 4 wt % NaX zeolite loading (Table 2) were prepared by the solution

Table 2. Dense Membranes and Mixed Matrix Membranes in NMP and CHCl$_3$

code	polymer	zeolite wt %	zeolite topology
2aA	2aA		
2aA-NaX4	2aA	4	FAU-NaX
2aB	2aB		
2aB-NaX4	2aB	4	FAU-NaX

casting method using NMP or CHCl$_3$ (2aA-NaX4, 2aB-NaX4) as solvents. Membrane thickness was controlled using a well-defined concentration of polymer–zeolite solution poured onto a 28.26 cm^2 glass plate (for NMP solutions) and metal rings (for CHCl$_3$ solutions) containing cellulose paper at the bottom to facilitate the removal of the membranes after solvent evaporation. Membranes in CHCl$_3$ were formed at room temperature after 24 h of solvent evaporation, whereas membranes in NMP were obtained inside a conventional oven at 80 °C as follows: a 7.5% w/v polymer solution was prepared by dissolving the polymer in NMP at room temperature, then the zeolite powder (4% wt zeolite/wt polymer) was added and stirred at room temperature for 1 h. To properly disperse the zeolite particles in the polymeric solution, the mixture was sonicated in an ultrasonic probe (50% sonication amplitude) for 5 min; then, the solution was cast onto a glass plate inside a conventional oven at 80 °C. The thickness values obtained for pristine membranes and MMMs in NMP were 65–85 and 85–125 μm, respectively. The obtained membranes were further dried in a vacuum oven as follows: 80 °C for 24 h, 150 °C for 24 h, and 200 °C for 24 h, to remove solvent remnants in the membranes. Finally, the membranes were cooled down to room temperature under vacuum conditions. Mixed matrix membranes in CHCl$_3$ were prepared as follows: a 2% w/v polymer solution was prepared

by dissolving the polymer in CHCl$_3$ at room temperature; then, the zeolite powder (4% wt zeolite/wt polymer) was added and stirred at room temperature for 1 h. The mixture was sonicated in an ultrasonic probe (50% sonication amplitude) for 3 min. Then, the mixture was cast onto a level surface in a glass ring cover with a watch glass to allow slow solvent evaporation at room temperature. The thickness values obtained for pristine membranes and MMMs in CHCl$_3$ were 30–40 and 65–125 μm, respectively. The obtained membranes were further dried in a vacuum oven at 80 °C for 24 h to remove solvent remnants.

Characterization Techniques. The morphology of the mixed matrix membranes was observed using a scanning electron microscope (HITACHI, SU3500) to analyze the MMMs and polymer membrane cross sections. The samples were fractured under cryogenic conditions prior to SEM measurements. Nuclear magnetic resonance (NMR) spectra were taken on Bruker Avance digital spectrometer, operating at 300 and 75 MHz for ^{1}H and ^{13}C, respectively. Chloroform-*d* (CDCl$_3$) was used as a solvent. Infrared (IR) spectra were measured on a Thermo Scientific Nicolet FT-IR-attenuated total reflection(ATR) spectrometer. The inherent viscosities of 0.2% polymer solutions in *N*-methyl-2-pyrrolidone (NMP) were measured at 25 °C using an Ubbelohde viscometer. The density and free fraction volume of dried pristine membranes were estimated at 30 °C in a density gradient column using a well-degassed aqueous zinc chloride solution, and then the densities were used to calculate the fractional free volume (FFV) using the following equation

$$\text{FFV} = \frac{V(30\,°\text{C}) - V(0)}{V(30\,°\text{C})} \tag{1}$$

where $V(30\,°\text{C})$ is the experimentally measured specific volume of the polymer at 30 °C and $V(0)$ is the occupied specific volume at 0 K, which can be estimated from the van der Waals volume (V_w) using the group contribution method developed by Van Krevelen[34] according to the relation $V(0) = 1.3 \sum V_w$. Permeability coefficients, $P(i)$, for ultrahigh-purity gases He, H$_2$, O$_2$, N$_2$, CH$_4$, and CO$_2$ of the neat polymer membranes and their MMMs were measured at 35 °C and 2 bar, in a variable-pressure/constant volume permeation cell following a procedure reported elsewhere.[42] Gas permeability coefficients for each gas, $P(i)$, were determined from the slope of the downstream pressure versus time plot once achieving steady state. The apparent diffusion coefficients, $D(i)$, and apparent solubility coefficients, $S(i)$, for each gas were calculated from the time lag $\theta(i)$ using the following equations

$$D(i) = \frac{L^2}{6\theta(i)} \tag{2}$$

$$S(i) = \frac{P(i)}{D(i)} \tag{3}$$

In eq 2, L is the film thickness; for this study, ideal selectivity for two gas pairs, i and j, is defined as the ratio of two pure gas permeability coefficients, $P(i)/P(j)$.

■ ASSOCIATED CONTENT

ⓢ Supporting Information

The Supporting Information is available free of charge at https://pubs.acs.org/doi/10.1021/acsomega.0c05978.

Pictures of FAU topology, SEM micrographs of the FAU zeolites and tables of elemental composition of the parent FAU zeolites, thermal properties of membranes of polymers 2aA and 2aB and MMMs, and apparent diffusivity coefficients and selectivity, as well as solubility coefficients and selectivity for different membranes based on 2aA and 2aB polymers and their MMMs (PDF)

■ AUTHOR INFORMATION

Corresponding Authors

Eduardo Coutino-Gonzalez − *Centro de Investigaciones en Óptica, A. C., León, Guanajuato 37150, México;* orcid.org/0000-0001-8296-0168; Email: ecoutino@cio.mx

Lilian Irais Olvera − *Instituto de Investigaciones en Materiales, Universidad Nacional Autónoma de México, 04510 Ciudad de México, México;* orcid.org/0000-0002-1505-2319; Email: lolvera@materiales.unam.mx

Authors

Hugo Hernández-Martínez − *Centro de Investigación y Desarrollo Tecnológico en Electroquímica, Parque Industrial Querétaro, Querétaro 76703, México;* orcid.org/0000-0002-5303-3215

Fabricio Espejel-Ayala − *Centro de Investigación y Desarrollo Tecnológico en Electroquímica, Parque Industrial Querétaro, Querétaro 76703, México*

Francisco Alberto Ruiz-Treviño − *Departamento de Ingeniería Química, Industrial y de Alimentos, Universidad Iberoamericana, Ciudad de México 01219, México;* orcid.org/0000-0002-6476-8137

Gabriel Guerrero-Heredia − *Departamento de Ingeniería Química, Industrial y de Alimentos, Universidad Iberoamericana, Ciudad de México 01219, México; Department of Chemical Engineering, Norwegian University of Science and Technology, 7491 Trondheim, Norway*

Ana Laura García-Riego − *Tecnológico de Estudios Superiores de San Felipe del Progreso, Avenida Instituto Tecnológico S/N, 50640 San Felipe del Progreso, México*

Complete contact information is available at:
https://pubs.acs.org/10.1021/acsomega.0c05978

Notes

The authors declare no competing financial interest.

■ REFERENCES

(1) Bernardo, P.; Drioli, E.; Golemme, G. Membrane gas separation: a review/state of the art. *Ind. Eng. Chem. Res.* **2009**, *48*, 4638−4663.

(2) Mohamed, M. J. B. G.; Mannan, H. A.; Nasir, R.; Mohshim, D. F.; Mukhtar, H.; Abdulrahman, A.; Ahmed, A. Composite mixed matrix membranes incorporating microporous carbon molecular sieve as filler in polyethersulfone for CO_2/CH_4 separation. *J. Appl. Polym. Sci* **2020**, *137*, No. 48476.

(3) Siagian, U. W. R.; Raksajati, A.; Himma, N. F.; Khoiruddin, K.; Wenten, I. G. Membrane-based carbon capture technologies: Membrane gas separation vs. membrane contactor. *J. Nat. Gas Sci. Eng.* **2019**, *67*, 172−195.

(4) Robeson, L. M. The upper bound revisited. *J. Membr. Sci* **2008**, *320*, 390−400.

(5) Nik, O. G.; Chen, X. Y.; Kaliaguine, S. Amine-functionalized zeolite FAU/EMT polyimide mixed matrix membranes for CO_2/CH_4 separation. *J. Membr. Sci.* **2011**, *379*, 468−478.

(6) Amooghin, A. E.; Mashhadikhan, S.; Sanaeepur, H.; Moghadassi, A.; Matsuura, T.; Ramakrishna, S. Substantial breakthroughs on function-led design of advanced materials used in mixed matrix membranes (MMMs): A new horizon for efficient CO_2 separation. *Prog. Mater. Sci.* **2019**, *102*, 222−295.

(7) Zarshenas, K.; Raisi, A.; Aroujalian, A. Mixed matrix membrane of nano-zeolite NaX/poly (ether-block-amide) for gas separation applications. *J. Membr. Sci* **2016**, *510*, 270−283.

(8) Huang, Z.; Li, Y.; Wen, R.; May Teoh, M.; Kulprathipanja, S. Enhanced gas separation properties by using nanostructured PES-Zeolite 4A mixed matrix membranes. *J. Appl. Polym. Sci* **2006**, *101*, 3800−3805.

(9) Hashemifard, S. A.; Ismail, A. F.; Matsuura, T. Mixed matrix membrane incorporated with large pore size halloysite nanotubes (HNT) as filler for gas separation: experimental. *J. Colloid Interface Sci.* **2011**, *359*, 359−370.

(10) Chung, T.-S.; Jiang, L. Y.; Li, Y.; Kulprathipanja, S. Mixed matrix membranes (MMMs) comprising organic polymers with dispersed inorganic fillers for gas separation. *Prog. Polym. Sci.* **2007**, *32*, 483−507.

(11) Adams, R. T.; Lee, J. S.; Bae, T. H.; Ward, J. K.; Johnson, J. R.; Jones, C. W.; Nair, S.; Koros, W. J. $CO_2−CH_4$ permeation in high zeolite 4A loading mixed matrix membranes. *J. Membr. Sci* **2011**, *367*, 197−203.

(12) Wang, X.; Ding, X.; Zhao, H.; Fu, J.; Xin, Q.; Zhang, Y. Pebax-based mixed matrix membranes containing hollow polypyrrole nanospheres with mesoporous shells for enhanced gas permeation performance. *J. Membr. Sci.* **2020**, *602*, No. 117968.

(13) Wolińska-Grabczyk, A.; Kubica, P.; Jankowski, A.; Wójtowicz, M.; Kansy, J.; Wojtyniak, M. Gas and water vapor transport properties of mixed matrix membranes containing 13X zeolite. *J. Membr. Sci.* **2017**, *526*, 334−347.

(14) Vermeiren, W.; Gilson, J. P. Impact of zeolites on the petroleum and petrochemical industry. *Top. Catal.* **2009**, *52*, 1131−1161.

(15) Inayat, A.; Schneider, C.; Schwieger, W. Organic-free synthesis of layer-like FAU-type zeolites. *Chem. Commun.* **2015**, *51*, 279−281.

(16) Salehi, S.; Anbia, M. Adsorption Selectivity of CO_2 and CH_4 on Novel PANI/Alkali-Exchanged FAU Zeolite Nanocomposites. *J. Inorg. Organomet. Polym. Mater.* **2017**, *27*, 1281−1291.

(17) Dargaville, T. R.; George, G. A.; Hill, D. J.; Whittaker, A. K. High energy radiation grafting of fluoropolymers. *Prog. Polym. Sci.* **2003**, *28*, 1355−1376.

(18) Olvera, L. I.; Guzmán-Gutiérrez, M. T.; Zolotukhin, M. G.; Fomine, S.; Cárdenas, J.; Ruiz-Trevino, F. A.; Villers, D.; Ezquerra, T. A.; Prokhorov, E. Novel high molecular weight aromatic fluorinated polymers from one-pot, metal-free step polymerizations. *Macromolecules* **2013**, *46*, 7245−7256.

(19) Yampolskii, Y.; Belov, N.; Alentiev, A. Perfluorinated polymers as materials of membranes for gas and vapor separation. *J. Membr. Sci.* **2020**, *598*, No. 117779.

(20) Odian, G. *Principles of Polymerization*, 4th ed.; John Wiley & Sons, 2004.

(21) Cruz, A. R.; Hernandez, M. C. G.; Guzmán-Gutiérrez, M. T.; Zolotukhin, M. G.; Fomine, S.; Morales, S. L.; Kricheldorf, H.; Wilks, E. S.; Cárdenas, J.; Salmón, M. Precision synthesis of narrow polydispersity, ultrahigh molecular weight linear aromatic polymers by

A2+ B2 nonstoichiometric step-selective polymerization. *Macromolecules* **2012**, *45*, 6774−6780.

(22) Abu-Zied, B. M. Cu²⁺-acetate exchanged X zeolites: Preparation, characterization and N₂O decomposition activity. *Microporous Mesoporous Mater.* **2011**, *139*, 59−66.

(23) Zheng, Y.; Wu, Y.; Zhang, B.; Wang, Z. Preparation and characterization of CO₂-selective Pebax/NaY mixed matrix membranes. *J. Appl. Polym. Sci.* **2020**, *137*, No. 48398.

(24) Car, A.; Stropnik, C.; Peinemann, K. V. Hybrid membrane materials with different metal-organic frameworks (MOFs) for gas separation. *Desalination* **2006**, *200*, 424−426.

(25) Husain, S.; Koros, W. J. Mixed matrix hollow fiber membranes made with modified HSSZ-13 zeolite in polyetherimide polymer matrix for gas separation. *J. Membr. Sci* **2007**, *288*, 195−207.

(26) Mahajan, R.; Koros, W. J. Factors controlling successful formation of mixed-matrix gas separation materials. *Ind. Eng. Chem. Res.* **2000**, *39*, 2692−2696.

(27) Mahajan, R.; Burns, R.; Schaeffer, M.; Koros, W. J. Challenges in forming successful mixed matrix membranes with rigid polymeric materials. *J. Appl. Polym. Sci.* **2002**, *86*, 881−890.

(28) Dong, G.; Li, H.; Chen, V. Challenges and opportunities for mixed-matrix membranes for gas separation. *J. Mater. Chem. A* **2013**, *1*, 4610−4630.

(29) Diaz, A. M.; Zolotukhin, M. G.; Fomine, S.; Salcedo, R.; Manero, O.; Cedillo, G.; Velasco, V. M.; Guzman, M. T.; Fritsch, D.; Khalizov, A. F. A novel, one-pot synthesis of novel 3F, 5F, and 8F aromatic polymers. *Macromol. Rapid Commun.* **2007**, *28*, 183−187.

(30) Sánchez-García, S.; Ruiz-Treviño, F. A.; Aguilar-Vega, M. J.; Zolotukhin, M. G. Gas permeability and selectivity in thermally modified poly (oxyindole biphenylylene) membranes bearing a tert-butyl carbonate group. *Ind. Eng. Chem. Res.* **2016**, *55*, 7012−7020.

(31) Hernández-Martínez, H.; Ruiz-Treviño, F. A.; Ortiz-Espinoza, J.; Aguilar-Vega, M. J.; Zolotukhin, M. G.; Marcial-Hernandez, R.; Olvera, L. I. Simultaneous thermal cross-linking and decomposition of side groups to mitigate physical aging in poly (oxyindole biphenylylene) gas separation membranes. *Ind. Eng. Chem. Res.* **2018**, *57*, 4640−4650.

(32) Ortiz-Espinoza, J.; Ruiz-Treviño, F. A.; Hernández-Martínez, H.; Aguilar-Vega, M. J.; Zolotukhin, M. G. Gas transport properties in cross-linked and vacuum annealed poly (oxyindole biphenylylene) membranes. *Ind. Eng. Chem. Res.* **2018**, *57*, 12511−12518.

(33) Mancilla, E. C.; Hernández-Martínez, H.; Zolotukhin, M. G.; Ruiz-Treviño, F. A.; González-Díaz, M. O.; Cardenas, J.; Scherf, U. POXINAR Membrane Family for Gas Separation. *Ind. Eng. Chem. Res.* **2019**, *58*, 15280−15287.

(34) Van Krevelen, D. W. *Properties of Polymers: Their Correlation with Chemical Structure, Their Numerical Estimation and Prediction from Additive Group Contributions*; Elsevier: Amsterdam, The Netherlands, 1960.

(35) Chong Lua, A.; Shen, Y. Influence of inorganic fillers on the structural and transport properties of mixed matrix membranes. *J. Appl. Polym. Sci.* **2013**, *128*, 4058−4066.

(36) Lee, W. H.; Park, E. J.; Han, J.; Shin, D. W.; Kim, Y. S.; Bae, C. Poly (terphenylene) anion exchange membranes: the effect of backbone structure on morphology and membrane property. *ACS Macro Lett.* **2017**, *6*, 566−570.

(37) Murali, R. S.; Sridhar, S.; Sankarshana, T.; Ravikumar, Y. V. L. Gas permeation behavior of Pebax-1657 nanocomposite membrane incorporated with multiwalled carbon nanotubes. *Ind. Eng. Chem. Res.* **2010**, *49*, 6530−6538.

(38) Paul, D. R.; Yampolskii, Y. *Polymeric Gas Separation Membranes*; CRC Press: Boca Raton, FL, 1994.

(39) Banerjee, S.; Maier, G.; Dannenberg, C.; Spinger, J. Gas permeabilities of novel poly (arylene ether) s with terphenyl unit in the main chain. *J. Membr. Sci.* **2004**, *229*, 63−71.

(40) Huang, Z.; Su, J. F.; Su, X. Q.; Guo, Y. H.; Teng, L. J.; Min Yang, C. Preparation and permeation characterization of β-zeolite-incorporated composite membranes. *J. Appl. Polym. Sci.* **2009**, *112*, 9−18.

(41) Azizi, N.; Mohammadi, T.; Behbahani, R. M. Comparison of permeability performance of PEBAX-1074/TiO₂, PEBAX-1074/SiO₂ and PEBAX-1074/Al₂O₃ nanocomposite membranes for CO₂/CH₄ separation. *Chem. Eng. Res. Des.* **2017**, *117*, 177−189.

(42) Camacho-Zuñiga, C.; Ruiz-Treviño, F. A.; Zolotukhin, M. G.; Del Castillo, L. F.; Guzman, J.; Chavez, J.; Torres, G.; Gileva, N. G.; Sedova, E. A. Gas transport properties of new aromatic cardo poly(aryl ether ketone)s. *J. Membr. Sci.* **2006**, *283*, 393−398.